

Published in final edited form as:

*Stem Cells*. 2012 July ; 30(7): 1477–1485. doi:10.1002/stem.1109.

## Paternally Inherited $Gs\alpha$ Mutation Impairs Adipogenesis and Potentiates a Lean Phenotype In Vivo

Jan-jan Liu<sup>a,b</sup>, Elizabeth Russell<sup>c</sup>, Deyu Zhang<sup>a,b</sup>, Frederick S. Kaplan<sup>a,b,c</sup>, Robert J. Pignolo<sup>a,b,c</sup>, and Eileen M. Shore<sup>a,b,d</sup>

<sup>a</sup>Department of Orthopaedic Surgery, Perelman School of Medicine, University of Pennsylvania, Philadelphia, Pennsylvania, USA

<sup>b</sup>Center for Research in FOP and Related Disorders, Perelman School of Medicine, University of Pennsylvania, Philadelphia, Pennsylvania, USA

<sup>c</sup>Department of Medicine, Perelman School of Medicine, University of Pennsylvania, Philadelphia, Pennsylvania, USA

<sup>d</sup>Department of Genetics, Perelman School of Medicine, University of Pennsylvania, Philadelphia, Pennsylvania, USA

### Abstract

Paternally inherited inactivating mutations of the *GNAS* gene have been associated with a rare and disabling genetic disorder, progressive osseous heteroplasia, in which heterotopic ossification occurs within extraskeletal soft tissues, such as skin, subcutaneous fat, and skeletal muscle. This ectopic bone formation is hypothesized to be caused by dysregulated mesenchymal progenitor cell differentiation that affects a bipotential osteogenic-adipogenic lineage cell fate switch.

Interestingly, patients with paternally inherited inactivating mutations of *GNAS* are uniformly lean. Using a mouse model of *Gs\alpha*-specific exon 1 disruption, we examined whether heterozygous inactivation of *Gnas* affects adipogenic differentiation of mesenchymal precursor cells from subcutaneous adipose tissues (fat pad). We found that paternally inherited *Gs\alpha* inactivation ( $Gs\alpha^{+/p-}$ ) impairs adipogenic differentiation of adipose-derived stromal cells (ASCs). The  $Gs\alpha^{+/p-}$  mutation in ASCs also decreased expression of the adipogenic factors CCAAT-enhancer-binding protein (*C/EBP*) $\beta$ , *C/EBP\alpha*, peroxisome proliferator-activated receptor gamma, and adipocyte protein 2. Impaired adipocyte differentiation was rescued by an adenylyl cyclase activator, forskolin, and provided evidence that *Gs\alpha*-cAMP signals are necessary in early stages of this process. Supporting a role for *Gnas* in adipogenesis in vivo, fat tissue weight and expression of adipogenic genes from multiple types of adipose tissues from  $Gs\alpha^{+/p-}$  mice were significantly

© AlphaMed Press

Correspondence: Robert J. Pignolo, M.D., Ph.D., Department of Medicine, Perelman School of Medicine at the University of Pennsylvania, 424 Stemmler Hall, 3450 Hamilton Walk, Philadelphia, Pennsylvania 19104-6081, USA. Telephone: 215-573-8138; pignolo@mail.med.upenn.edu; or Eileen M. Shore, Ph.D., Department of Orthopaedic Surgery, Perelman School of Medicine at the University of Pennsylvania, 426A Stemmler Hall, 3450 Hamilton Walk, Philadelphia, Pennsylvania 19104-6081, USA. Telephone: 215-898-2331; Fax: 215-573-2133; shore@mail.med.upenn.edu.

### Disclosure of Potential Conflicts of Interest

The authors indicate no potential conflicts of interest.

Author contributions: J.-J.L.: experimental design, collection and/or assembly of data, data analysis and interpretation, manuscript writing, and final approval of manuscript; E.R.: collection and/or assembly of data, data analysis and interpretation, manuscript writing, and final approval of manuscript; D.Z.: provision of study materials and final approval of manuscript; F.S.K.: data analysis and interpretation, manuscript writing, and final approval of manuscript; R.J.P.: conception and design, financial support, collection and/or assembly of data, data analysis and interpretation, manuscript writing, and final approval of manuscript; E.M.S.: conception and design, financial support, data analysis and interpretation, manuscript writing, and final approval of manuscript. R.J.P. and E.M.S. contributed equally to this article.

decreased. Interestingly, the inhibition of adipogenesis by paternally inherited *Gsa* mutation also enhances expression of the osteogenic factors, msh homeobox 2, runt-related transcription factor 2, and osteocalcin. These data support the hypothesis that *Gsa* plays a critical role in regulating the balance between fat and bone determination in soft tissues, a finding that has important implications for a wide variety of disorders of osteogenesis and adipogenesis.

## Keywords

GNAS; Progressive osseous heteroplasia; Heterotopic ossification; Adipogenesis; Differentiation; Stem cells

## Introduction

Progressive osseous heteroplasia (POH) is a rare disorder of bone formation characterized by heterotopic ossification (HO) that forms in skin and subcutaneous tissues with subsequent progression into deep connective tissues, such as skeletal muscles, tendons, and ligaments [1, 2]. Considerable evidence supports the existence of bipotential progenitor cells that can give rise to osteoblasts and adipocytes [3–9]. In POH patients, intramembranous bone formation is frequently observed to initiate within the subcutaneous fat tissue suggesting a close, perhaps reciprocal, relationship between adipogenesis and osteogenesis in peripheral tissues that is mediated by a common connective tissue progenitor cell [10, 11].

Heterozygous inactivating mutations in the *GNAS* gene have been identified as a cause of POH [11]. The *GNAS* locus encodes multiple mRNAs [2, 12–14] with distinct first exons that splice into a set of common downstream exons (exon 2–13). Transcripts include those for *Gsa*, a subunit of the heterotrimeric G-protein that couples heptahelical receptors for many hormones and neurotransmitters to adenylyl cyclase activation and cAMP production. Heterotrimeric G-proteins, composed of  $\alpha$ ,  $\beta$ , and  $\gamma$  subunits, couple extracellular signals from specific cell surface receptors to intracellular effectors [12, 15]. G-proteins bind guanine nucleotides and are defined by the  $\alpha$ -subunit of the complex. In addition to *Gsa*, *GNAS* encodes *XLas*, which functions similarly as *Gsa* [16], and the chromogranin-like protein, NESP55 [17] as well as noncoding transcripts. Importantly, the *GNAS* locus is imprinted, resulting in differential RNA expression patterns that are determined by the parent from whom a *GNAS* allele is inherited [12–14].

Experimental evidence supports that *GNAS* mutations in POH occur on the paternally inherited *GNAS* allele [11]. Our previous investigation of human disorders of *GNAS*-associated HO noted that individuals with paternally inherited inactivating mutations of *GNAS* were uniformly lean [18], suggesting that fat stores may be regulated by specific parental allele expression of *GNAS* in humans [18, 19]. Such a parent-of-origin effect is reflected by the distinctly different clinical disorders that are caused by maternally inherited inactivating mutations of *GNAS* (e.g., pseudohypoparathyroidism 1A) [18, 20] that are associated with obesity. These observations further support that adipocyte differentiation and function might be regulated by allele-specific expression of *GNAS*.

Adipose tissues contain multipotential progenitor cells that can differentiate into adipocytes and osteoblasts under appropriate conditions [21, 22], and the distribution of HO in POH suggests that progenitor cells in subcutaneous, dermal, and intramuscular fat differentiate preferentially along an osteogenic lineage in response to inactivating mutations of the paternally inherited *GNAS* allele [23]. Previously, we have demonstrated that mesenchymal progenitor cells from adipose tissue with *GNAS* paternal allele inactivation show enhanced

osteogenesis [23]. In this study, we examine whether paternally inherited inactivation of *GNAS* impairs adipogenesis and the formation of fat tissue in vivo.

## Materials and Methods

### Patients/Human Subjects

The charts of 42 individuals who presented to the University of Pennsylvania Orthopaedic Surgery Outpatient Clinic for evaluation of nontraumatic HO of the skin and subcutaneous tissues who met diagnostic criteria for POH [18] were reviewed for documented birth weight and confirmed *GNAS* mutations. The study was approved by the Institutional Review Board of the University of Pennsylvania.

### Animals

Male mice carrying a heterozygous deletion in exon 1 of *Gnas* ( $Gsa^{+/P-}$ ; [24, 25]) were bred to CD1 female mice to maintain the deletion mutation on the paternally inherited allele. All studies were performed in 3-month-old male mice. (No data support that a paternally inherited mutation is reflected as different phenotypes in male and female progeny; however, a single gender was used to minimize any potential variability.) Animal experiments were approved by the Institutional Animal Care and Use Committee, University of Pennsylvania.

### Isolation and Culture of Adipose Soft Tissue Stromal Cells

Adipose-derived stromal cells (ASCs) from fat pads that overlie the pelvis and proximal femurs (subcutaneous adipose tissue; Supporting Information Fig. S2) from wild-type (WT) and  $Gsa^{+/P-}$  mice were isolated as previously described [23]. Briefly, fat pads were excised, washed with 1× phosphate buffered saline (PBS) and minced into small pieces. Minced fat tissue was digested with type II collagenase (Sigma, St. Louis, MO, [www.sigmaaldrich.com](http://www.sigmaaldrich.com)) for 1 hour with shaking in 37°C. After digestion, Dulbecco's modified Eagle's medium (DMEM)/F12 (with 10% fetal calf serum (FCS) and antibiotics) was added to neutralize the enzymatic activity of type II collagenase. The cell suspension was filtered through a 100- $\mu$ M cell strainer (BD Biosciences, Franklin Lakes, NJ, [www.bdbiosciences.com](http://www.bdbiosciences.com)), recovered by centrifugation at 300g for 10 minutes, and then plated in growth medium containing DMEM/F12, 15%–20% FCS, and antibiotics during the first 2 days. After expansion, the cells were maintained in DMEM/F12 containing 10% FCS and antibiotics. ASCs from abdominal white adipose tissue (WAT) and interscapular brown adipose tissue (BAT) were isolated (Supporting Information Fig. S2) and processed as above, except the time for collagenase digestion was reduced to 20–30 minutes. Adherent cell strains were established from individual animals; cell strains from each single mouse were used at passage 3 or lower for all experiments and analyzed in triplicate; data in each experiment were from at least three individual mouse cell strains. The ability of ASCs to differentiate along adipogenic and osteogenic lineages was confirmed.

### Adipogenic Differentiation In Vitro

For adipogenic differentiation, ASCs from fat pads, WAT, or BAT were plated at a density of 20,000 per square centimeter and allowed to attach overnight in growth media. The cells from fat pads and WAT were grown to confluence and then induced to adipocyte differentiation with medium containing DMEM/F12 growth media supplemented with 10  $\mu$ g/ml insulin, 10 ng/ml 3',3',5' triiodo-L-thyronine (T3), 1  $\mu$ M dexamethasone (all from Sigma), and 0.2  $\mu$ M (fat pads) or 0.5  $\mu$ M (WAT) rosiglitazone (Cayman Chemical, Ann Arbor, MI, [www.caymanchem.com](http://www.caymanchem.com)). Cells were harvested at indicated time points for total RNA isolation to quantify the expression of lipid marker genes and for lipid detection. ASCs

from interscapular BAT were pretreated with 100 ng/ml rhBMP7 (R&D Systems, Minneapolis, MN, [www.rndsystems.com](http://www.rndsystems.com)) for 3–4 days upon confluence, then induced to adipocyte differentiation in DMEM/F12 media containing 10% FCS supplemented with 10  $\mu$ g/ml insulin, 10 ng/ml T3, 1  $\mu$ M dexamethasone, and 0.2  $\mu$ M rosiglitazone for an additional 7 days. To activate adenylyl cyclase, ASCs from fat pads were treated with forskolin (10 ng/ml in dimethyl sulfoxide (DMSO)) as indicated in Figure 3.

### RNA Isolation and Relative Quantitative Reverse-Transcriptase Polymerase Chain Reaction

Quantitative reverse-transcriptase polymerase chain reaction (qRT-PCR) analysis used standard methods. Total RNA was extracted from cells at specific time points using the TRIzol Reagent (Invitrogen, Grand Island, NY, <http://www.invitrogen.com>) and MiniRNeasy (Qiagen, Valencia, CA, <http://www1.qiagen.com>), according to the manufacture's instructions. Complementary DNA synthesis was carried out on 2–5  $\mu$ g of total RNA per sample using the Superscript III RT kit (Invitrogen) following the manufacture's instructions. Transcripts were amplified and their levels were quantified using gene-specific primers (primer pairs listed in Supporting Information Table S1) and Fast SYBR Green Master Mix (Applied Biosystems, Carlsbad, CA, [www.appliedbiosystems.com](http://www.appliedbiosystems.com)) on the ABI 7500 Fast Real Time PCR System (Applied Biosystems). At least three biological replicates were performed for each transcript and measurements were made in triplicate per each sample; no-template samples served as negative controls. Gene expression was normalized to TATA box binding protein,  $\beta$ -actin, and/or  $\beta_2$ -microglobulin as an internal standard, and the average of WT day 0 without induction was set to 1 ( $n = 3$  per group).

### Oil Red O Staining

Following adipogenic induction, cells were fixed in 10% formalin for 1 hour and stained with 60% oil red O (Sigma) for 10 minutes. For quantification, oil red O was solubilized in 100% isopropanol and the optical absorbance measured at 500 nm using a Bio-Rad microplate reader. Results were normalized to total protein content (BCA protein assay; Pierce, Rockford, IL, [www.piercenet.com](http://www.piercenet.com)).

### Anthropomorphic and Gross Tissue Measurements

Upon sacrifice, 3-month-old mice (that had been maintained on a standard chow diet; NIH-07, 5% fat by weight) were weighed, and their length measured as the distance from nose to the base of the tail. Body mass index (BMI) was used to evaluate adiposity [26] and calculated according to the formula  $BMI = \text{mass (g)} / (\text{length [cm]})^2$ . WAT was dissected from the intra-abdominal region, BAT from the interscapular region, and fat pads from the subcutaneous areas that overlie the proximal femurs. The excised tissues were weighed immediately upon dissection.

### Histology and Histomorphometry

Fat pads, BAT, and WAT were frozen at  $-40^{\circ}\text{C}$  in tissue freezing medium (Triangle Biomedical Sciences, Durham, NC, [www.trianglebiomedical.com](http://www.trianglebiomedical.com)). Frozen tissue sections were cut at the following thicknesses: 6  $\mu$ m (brown fat), 8  $\mu$ m (fat pads), and 12  $\mu$ m (white fat). Sections were stained with hematoxylin and eosin by standard techniques. ImageJ software (Rasband, W.S., U.S. National Institutes of Health, Bethesda, MD, <http://rsb.info.nih.gov/ij/>) was used to analyze the mean adipocyte size (AS) and percent stroma. Briefly, images of stained sections were converted into tricolor images using Adobe Photoshop, with stroma, nuclei, and lipid (approximated as total cell contents with nuclei excluded) represented as different colors. After normalizing ImageJ and microscopy unit

scales, areas representing each of the three morphologic regions were quantified by ImageJ within randomly selected regions of interest (ROIs) and the number of cells within each ROI was counted. Average AS (Avg. AS) within ROIs was calculated as: Avg. AS = (Area of cell contents [lipid] + nuclear area)/total number of adipocytes. Stroma area (StrA) was calculated as: StrA = ROI area – area occupied by adipocytes. The percent stroma (% Str) was calculated as: % Str = (Area occupied by stroma/total ROI area) × 100.

### Statistical Analysis

The *t* test (Student's *t* test, two-sided, and paired) was used to determine whether the mean value for relative transcript expression in cells differed significantly between groups with and without adipogenic differentiation, between WT and mutant mice upon adipogenic differentiation and between groups with or without forskolin treatment. The *t* test was also used to determine whether weight, length, BMI, and weights of gross adipose tissues significantly differed between WT and *Gsa*<sup>+/-</sup> animals and to determine whether the average AS or percent stroma from ROIs in brown fat, white fat, and fat pads were significantly different between WT and *Gsa*<sup>+/-</sup> animals. Significance was set to \*, *p* < .05; \*\*, *p* < .01; and \*\*\*, *p* < .001. All statistical calculations were performed using Microsoft Excel. Unless otherwise indicated, data are shown as mean ± SE of the mean (*n* = 3 per group).

## Results

### POH Patients Have Decreased Adiposity and Low Birth Weights

Paternally inherited inactivating *GNAS* mutations have been identified in patients with POH [11, 27]. We reviewed the available birth weights of 13 patients with POH and found that three of four males and seven of nine females had measurements at or below the fifth percentile compared to sex-matched normative data (Supporting Information Fig. S1). All patients had POH by clinical diagnostic criteria, were lean at the time of initial presentation, and all but one had confirmed inactivating *GNAS* mutations.

### Paternally Inherited *Gsa* Inactivating Mutation Impairs Adipogenic Differentiation In Vitro

The low birth weights in patients with POH prompted us to investigate the effects on adipogenesis of reduced *Gsa* expression that results from paternal allele inactivation. During normal adipose development, adipocytes arise from precursor cells in the vascular stroma of fat tissue [28]. Subcutaneous adipose tissue is a frequent location of HO initiation in POH patients; therefore, we isolated murine ASCs from subcutaneous fat pad depots (Supporting Information Fig. S2A) of heterozygous knockout mice with a paternally inherited inactivating mutation of the *Gsa* transcript-specific exon 1 in *Gnas* (*Gsa*<sup>+/-</sup>) [23, 29].

Under conditions of adipogenic induction, ASC cells derived from subcutaneous fat pads of WT littermates efficiently differentiated into adipocytes (Fig. 1A, 1B) as indicated by lipid detection with oil red O staining to quantify neutral triglycerides. *Gsa*<sup>+/-</sup> ASCs had significantly less lipid accumulation compared to WT ASCs (Fig. 1A, 1B), indicating impaired adipocyte differentiation. In our previous studies [23], we did not detect any difference in the proliferation rates between *Gsa*<sup>+/-</sup> and WT ASCs by BrdU pulse labeling, excluding that impaired adipogenesis in *Gsa*<sup>+/-</sup> cells results from reduced numbers of precursor cells.

Adipogenesis is regulated through multiple transcription factors, including peroxisome proliferator-activated receptor gamma (PPAR $\gamma$ ) and CCAAT-enhancer-binding proteins (C/EBPs) [30]. We examined the expression of C/EBP $\beta$ , C/EBP $\alpha$ , and PPAR $\gamma$  as well as



adipocyte protein 2 (aP2, also called fatty acid binding protein 4), a marker for mature adipocytes, in WT and *Gsa*<sup>+/-</sup> ASCs by qRT-PCR. All of these transcripts were induced upon adipocyte differentiation of WT and *Gsa*<sup>+/-</sup> ASCs; however, the mutant cells showed a lower level of upregulated expression (Fig. 1C) supporting that inactivation of the paternally inherited *Gsa* allele impairs adipogenic differentiation.

### **Gnas Transcripts are Differentially Expressed During Adipocyte Differentiation and in Response to Paternally Inherited *Gsa* Mutation**

In both mouse and humans, *Gnas/GNAS* is a complex gene locus that encodes several transcripts including the biallelically expressed *Gsa*, paternal allele-specific XLAs, and maternal allele-specific Nesp (known as NESP55 in human). We quantified the levels of three transcripts (*Gsa*, XLAs, and Nesp) during adipogenesis of mouse ASCs and found that during initial stages of differentiation, *Gsa* and XLAs transcripts were reduced in *Gsa*<sup>+/-</sup> ASCs compared to WT ASCs (Fig. 2A, 2B). By contrast, the Nesp transcript was detected at a statistically significant higher level in *Gsa*<sup>+/-</sup> mutant ASCs prior to adipogenic differentiation (Fig. 2C). These data support that in addition to decreased expression of *Gsa* in cells from a *Gsa*<sup>+/-</sup> exon 1-specific knockout, inactivation of *Gsa* in this model also influences the expression of other transcripts within the *Gnas* locus—reducing the paternal allele-specific XLAs transcript early after differentiation and increasing the maternal allele-specific Nesp transcript at baseline.

### **Adenylyl Cyclase Activation at Early Stages of Differentiation Rescues the Impaired Adipogenesis of *Gsa* Inactivating Mutation**

Activation of heterotrimeric G-proteins promotes the binding of GTP to their  $\alpha$  subunits (*Gsa*), and subsequently activate downstream intracellular effectors, including second messenger enzyme (adenylyl cyclase), protein kinases (PKA and PKC), and ion channels [12, 19]. Adipogenesis has previously been shown to be regulated by *Gsa* and cAMP signaling [31–34]. To investigate whether the impaired adipogenesis by *Gsa*<sup>+/-</sup> ASCs is dependent on decreased cAMP signaling, cells were treated with an adenylyl cyclase activator, forskolin. Subcutaneous fat pad ASCs were induced with adipogenic media and treated with forskolin at an early differentiation stage (days 1 and 2 postinduction) or at a later stage (days 5 and 6 postinduction) and then assessed by oil red O staining on day 10 (Fig. 3). Forskolin treatment during days 5 and 6 had little effect on *Gsa*<sup>+/-</sup> impaired adipogenesis; however, treatment during days 1 and 2 restored the adipogenic deficiency in *Gsa*<sup>+/-</sup> ASCs (Fig. 3). Although we cannot exclude the possibility that another activation pathway, in addition to or as an alternative to cAMP, is involved in this process, these data support that *Gsa* enhances adipogenesis through generation of cAMP during early stages of adipogenic differentiation. Forskolin cannot induce adipocyte differentiation in the absence of adipogenic inducers, indicating that other factors are required in addition to cAMP. Our data support that early factors coordinate adipogenic differentiation and that *Gsa*-cAMP signals are necessary for this differentiation process.

### **Inactivating *Gsa* Mutation Reduces Abundance of Adipose Tissues In Vivo**

To examine the effects of *Gsa* inactivation on adipogenesis in vivo, we examined three sources of adipose tissues: subcutaneous fat pad, intra-abdominal WAT (visceral WAT), and interscapular BAT (Supporting Information Fig. S2A). We found all three sources of fat tissues reduced in size in *Gsa*<sup>+/-</sup> mice compared to control littermates (Fig. 4A; Supporting Information Fig. S2B). Adipose tissue weights from the subcutaneous fat pads, intra-abdominal WAT, and interscapular BAT were reduced in *Gsa*<sup>+/-</sup> mice by 50.0%, 45.0%, and 59.8%, respectively (Table 1). This amount of fat in *Gsa*<sup>+/-</sup> mice is disproportionately lower compared to measured decreases in total body weight and body length that were reduced by 19.7% and 6.4%, respectively, in mutant mice compared to control littermates

(Table 1). This is reflected by calculated BMI (weight/length<sup>2</sup>) that was not statistically significantly different between *Gsa*<sup>+/-</sup> and control littermates, suggesting that the reduced fat content in *Gsa*<sup>+/-</sup> mice is not simply a reflection of proportionally reduced body mass. Although the weights of the fat tissues were reduced in *Gsa*<sup>+/-</sup> mice, histomorphologic examination of the fat tissues showed statistically significant increases in total adipocyte number per unit area (Table 2) and a smaller AS in *Gsa*<sup>+/-</sup> mice (Table 2 and Fig. 4A).

The expression of adipose marker genes in fat tissues was examined by qRT-PCR analysis. Consistent with in vitro data showing decreased levels of adipogenic markers in *Gsa*<sup>+/-</sup> ASCs isolated from fat pads (Fig. 1), subcutaneous fat pad adipose tissue from *Gsa*<sup>+/-</sup> mice showed decreased PPAR $\gamma$  and leptin (a WAT marker) (Fig. 4B). Expression of PPAR $\gamma$  and leptin was also reduced in abdominal WAT tissue from *Gsa*<sup>+/-</sup> mice (Fig. 4B). Interscapular BAT tissue showed decreased leptin and aP2; however, uncoupling protein 1, a BAT-specific marker, was unchanged in the brown fat from *Gsa*<sup>+/-</sup> mice (Fig. 4B). Thus, the paternally inherited *Gsa* mutation suppressed the expression of WAT-associated transcripts in vivo. Similarly to ASCs from subcutaneous fat pads, *Gsa*<sup>+/-</sup> ASCs derived from abdominal WAT or from interscapular BAT showed reductions in expression of markers of adipogenesis compared to WT ASCs (data not shown), indicating that *Gsa*<sup>+/-</sup> inactivating mutation impairs adipogenesis in multiple types of fat tissues.

### Paternally Inherited *Gsa* Mutation Potentiates Osteogenesis Over Adipogenesis

The formation of heterotopic intramembranous ossification frequently initiates within subcutaneous fat in patients with POH [1, 2], suggesting that adipocyte precursor cells could aberrantly differentiate along an osteogenic lineage. We examined the expression of osteogenic markers in ASCs of subcutaneous fat pads from *Gsa*<sup>+/-</sup> mice under conditions of adipogenic differentiation. Msh homeobox 2, an early osteogenic marker, runt-related transcription factor 2, an osteogenic transcription factor, and osteocalcin, a marker of terminal osteogenic differentiation were all expressed at higher levels in *Gsa*<sup>+/-</sup> ASCs during adipogenic induction compared to WT ASCs (Fig. 5). Neither mutant nor WT cells showed positive Alizarin red staining after 14 days (data not shown) indicating that these adipogenic conditions cannot support mineralization even in the presence of the *Gsa*<sup>+/-</sup> mutation. These data suggest that inhibition of adipogenesis by paternally inherited *Gsa* mutation enhances osteogenic potential by directly or indirectly promoting osteoblastogenesis, even in the presence of adipogenic inducing factors.

## Discussion

In a *Gnas* knockout mouse model of *Gsa*-specific exon 1 disruption, we found that paternally inherited *Gsa* inactivating mutation (*Gsa*<sup>+/-</sup>) impairs adipogenic differentiation of ASCs from subcutaneous fat tissue by decreasing the expression of adipogenic transcription factors C/EBP $\beta$ , C/EBP $\alpha$ , and PPAR $\gamma$ . Rescue of impaired adipocyte differentiation by an adenylyl cyclase activator indicates that *Gsa*-cAMP signals are necessary in the early stages of this process. In vivo, we observed a significant decrease in fat tissues and in expression of adipogenic genes from multiple adipose sources in *Gsa*<sup>+/-</sup> mice, suggesting that *Gsa* may be an obesity risk factor. Importantly, inhibition of adipogenesis by a paternally inherited *Gsa* mutation also potentiates osteogenesis by enhancing expression of osteogenic factors. Thus, *Gsa* plays a critical role in regulating lineage determination in soft tissue progenitor cells between adipogenic and osteogenic fates.

We previously identified paternally inherited inactivating mutations in the human *GNAS* gene as a cause of POH [11]. The main product of the *GNAS* gene is the  $\alpha$ -subunit of the stimulatory G-protein (*Gsa*). However, multiple RNAs are transcribed from different

promoters at the *GNAS* locus and the *GNAS* gene locus is imprinted, showing differential expression patterns of these transcripts from maternal versus paternal alleles [12–14]. Our previous studies of *GNAS*-based human disorders of HO demonstrated that POH patients with paternally inherited inactivating *GNAS* mutations were never obese [18], suggesting that leanness may be related to parental allele expression of *GNAS*.

Parent-of-origin metabolic effects of *Gnas* mutations have been examined in mouse *Gnas* knockout models [24, 35–37]. Mice with mutations of *Gnas* exon 2 (*E2*), an exon common to all protein-coding *Gnas* transcripts including *Gsa* and *XLas*, showed reciprocal changes in energy metabolism depending on the presence of mutations in either the paternal (*E2<sup>+/-</sup>*) or maternal (*E2<sup>m-/-</sup>*) allele [36, 37]. *E2<sup>+/-</sup>* mice had a severely lean phenotype with strikingly increased glucose tolerance, insulin sensitivity, and sympathetic nervous system activity. In contrast, *E2<sup>m-/-</sup>* mice developed obesity with increased lipid accumulation in BAT and WAT and associated with increased serum leptin level but lowered energy expenditure.

Similarly to the phenotype of mice, we observed global losses in fat from multiple adipose tissues in *Gsa<sup>+/-</sup>* mice with the accumulated fat from each source of adipose tissue in *Gsa<sup>+/-</sup>* mice markedly reduced compared to that derived from WT mice. *Gsa<sup>+/-</sup>* mice had a greater number of adipocytes per unit area, although these adipocytes were smaller in size. The defect in adipogenic differentiation by *Gsa<sup>+/-</sup>* ASCs is thus reflected in both the decreased amount of fat tissue and in the inability of adipocytes to accumulate lipid.

Other studies in *Gsa*-specific knockout mice in which *Gsa* exon 1 was deleted (*E1<sup>-</sup>*) have confirmed that adiposity is related to *Gsa* mutation from the paternal allele [24, 35]. Consistent with our findings, Germain-Lee et al. reported that *Gsa<sup>+/-</sup>* mice had a lean phenotype compared to *Gsa<sup>m-/-</sup>* mice [24] and observed normal hormonal responsiveness in *Gsa<sup>+/-</sup>* mice, consistent with our clinical findings in POH patients [18]. Interestingly, Chen et al., using a different exon 1 deletion, described their *E1<sup>+/-</sup>* mice as mildly obese and insulin resistant [18, 35]. Compared to the *E1<sup>+/-</sup>* mice model, the more limited exon 1 disruption in *Gsa<sup>+/-</sup>* mice used in our and the Germain-Lee studies recapitulates the leanness observed in POH patients and implicates *Gnas* imprinting as a requirement for metabolic consequences of paternally inherited *Gsa* exon 1 mutations.

Of interest, we observed that subcutaneous fat pad ASCs from *Gsa<sup>+/-</sup>* mice not only have decreased *Gsa* mRNA expression, as expected, but also show altered expression of other *Gnas* transcripts, an unexpected finding since the deletion only includes the *Gsa*-specific exon 1. Mice with paternal allele deletion of *XLas* (*Gnasxl<sup>+/-</sup>*) have a phenotype similar to *E2<sup>+/-</sup>* mice, with a lean phenotype and reduced lipid accumulation in adipose tissues [38, 39]. During osteogenesis [23] and during adipogenesis (this study), ASCs from *Gsa<sup>+/-</sup>* mice expressed reduced levels of *XLas* and *Gsa* mRNAs relative to WT ASCs undergoing differentiation, suggesting that the altered regulation of adipogenic and osteogenic differentiation in these mice could be a combined effect of both of these G-protein subunit isoforms.

The role of cAMP signaling in adipogenesis has been well established to directly induce the expression of *CEBPA* and *PPAR $\gamma$* , central transcriptional regulators of adipogenesis [30–34]. Consistently, we found that induction of adipogenesis requires activation of adenylyl cyclase and that deficits in adipogenic differentiation in ASCs from *Gsa<sup>+/-</sup>* mice can be rescued by an adenylyl cyclase activator.

The effect of cAMP activation/inhibition in osteogenesis has also been examined, with most studies reporting a requirement for increased cAMP during osteogenesis [40–46]. However, these studies were conducted in preosteoblastic cells that were already committed to the



osteoblast lineage. By contrast, our previous studies as well as other reports [23, 47–50] indicate that low cAMP levels and low *GNAS*/*Gnas* expression may be required to commit a progenitor cell to the osteogenic lineage.

Recently, *Gsa*<sup>+/*p*-</sup> mice have been reported to form subcutaneous heterotopic bone [23, 29]. Although the specific cell targets involved in HO and leanness in POH are unknown, investigation of bipotential osteoblast/adipocyte progenitors (such as ASCs) with inactivating *Gnas* mutations has direct implications for understanding this reciprocal phenotype in POH. We report here that ASCs from murine subcutaneous fat pads (adipose tissue intimately associated with cutaneous tissue and underlying fascia) show enhanced osteogenic differentiation, even in the presence of adipogenic induction factors, and impaired adipogenic differentiation when derived from *Gsa*<sup>+/*p*-</sup> mice, suggesting that they are relevant target cells that contribute to ectopic osteogenesis in POH patients. Our data show that cells with a paternally inherited *Gnas* mutation express osteogenic markers even in the presence of adipogenic factors, perhaps reflecting the tendency of mutant progenitor cells in POH patients to undergo ectopic osteogenesis. The levels of osteogenic marker expression was comparable to levels induced by ASCs under osteogenic conditions [23]; however, the cells did not mineralize under our adipogenic culture conditions. This suggests that the *Gsa*<sup>+/*p*-</sup> mutation may promote but not be sufficient to induce osteogenesis and may be reflected in the mosaic distribution of areas of HO in POH.

Extraskelatal bone formation in POH patients often arises within subcutaneous fat, suggesting a close, perhaps reciprocal, relationship between bone and fat cell differentiation. Taken together with existing reports, our data support the hypothesis that heterozygous inactivation of the *GNAS* gene alters cellular signaling in ASCs leading not only to ectopic osteogenesis but also to dramatically impaired adipogenesis. This study indicates that *GNAS*-regulated signaling directs bipotent osteoblast and adipocyte differentiation, demonstrates the complex phenotypic consequences of inactivating *GNAS* mutations that are regulated by maternal/paternal inheritance of *GNAS*, and suggests that lineage switching between osteogenic and adipogenic fates in fat tissue may be a therapeutic target in POH.

## Summary

Paternally inherited heterozygous inactivation of *Gnas* impairs adipogenic differentiation of mesenchymal progenitor cells from subcutaneous adipose tissues by early dysregulation of *Gsa*-cAMP signaling. Deficits in adipogenic differentiation result in a significant reduction of fat depots from multiple adipose tissues in *Gsa*<sup>+/*p*-</sup> mice. *Gsa* appears to be an important determinant of the balance between fat and bone determination in soft tissues.

## Acknowledgments

We acknowledge Michael Levine and Emily Germain-Lee for the generous gift of *Gnas*<sup>+/-</sup> mice. We also thank the members of our research laboratory, especially Meiqi Xu, Shengliang Zhang, Robert Caron, and Josef Kaplan for their thoughtful comments, assistance, and suggestions during the course of this work. This study was supported by the National Institutes of Health (NIH R01-AR046831 and ARRA R01-AR046831-S1), the Progressive Osseous Heteroplasia Association (POHA), the Italian POH Association, the International Fibrodysplasia Ossificans Progressiva Association (IFOPA), the University of Pennsylvania Center for Research in FOP and Related Disorders, the Penn Center for Musculoskeletal Disorders (NIH P30-AR050950), and the Isaac and Rose Nassau Professorship of Orthopaedic Molecular Medicine (F.S.K.).

## References

1. Kaplan FS, Shore EM. Progressive osseous heteroplasia. *J Bone Miner Res.* 2000; 15:2084–2094. [PubMed: 11092391]

2. Shore EM, Kaplan FS. Inherited human diseases of heterotopic bone formation. *Nat Rev Rheumatol.* 2010; 6:518–527. [PubMed: 20703219]
3. Ahdjoudj S, Lasmoles F, Oyajobi BO, et al. Reciprocal control of osteoblast/chondroblast and osteoblast/adipocyte differentiation of multipotential clonal human marrow stromal F/STRO-1(+) cells. *J Cell Biochem.* 2001; 81:23–38. [PubMed: 11180395]
4. Davis LA, Zur Nieden NI. Mesodermal fate decisions of a stem cell: The Wnt switch. *Cell Mol Life Sci.* 2008; 65:2658–2674. [PubMed: 18528633]
5. Gori F, Thomas T, Hicok KC, et al. Differentiation of human marrow stromal precursor cells: Bone morphogenetic protein-2 increases OSF2/CBFA1, enhances osteoblast commitment, and inhibits late adipocyte maturation. *J Bone Miner Res.* 1999; 14:1522–1535. [PubMed: 10469280]
6. Nuttall ME, Gimble JM. Is there a therapeutic opportunity to either prevent or treat osteopenic disorders by inhibiting marrow adipogenesis? *Bone.* 2000; 27:177–184. [PubMed: 10913909]
7. Nuttall ME, Patton AJ, Olivera DL, et al. Human trabecular bone cells are able to express both osteoblastic and adipocytic phenotype: Implications for osteopenic disorders. *J Bone Miner Res.* 1998; 13:371–382. [PubMed: 9525337]
8. Sabatakos G, Sims NA, Chen J, et al. Overexpression of DeltaFosB transcription factor(s) increases bone formation and inhibits adipogenesis. *Nat Med.* 2000; 6:985–990. [PubMed: 10973317]
9. Spinella-Jaegle S, Rawadi G, Kawai S, et al. Sonic hedgehog increases the commitment of pluripotent mesenchymal cells into the osteoblastic lineage and abolishes adipocytic differentiation. *J Cell Sci.* 2001; 114:2085–2094. [PubMed: 11493644]
10. Kaplan FS, Craver R, MacEwen GD, et al. Progressive osseous heteroplasia: A distinct developmental disorder of heterotopic ossification. Two new case reports and follow-up of three previously reported cases. *J Bone Joint Surg Am.* 1994; 76:425–436. [PubMed: 8126048]
11. Shore EM, Ahn J, de Beur SJ, et al. Paternally inherited inactivating mutations of the GNAS1 gene in progressive osseous heteroplasia. *N Eng J Med.* 2002; 346:99–106.
12. Plagge A, Kelsey G, Germain-Lee EL. Physiological functions of the imprinted Gnas locus and its protein variants Galpha(s) and XLalpha(s) in human and mouse. *J Endocrinol.* 2008; 196:193–214. [PubMed: 18252944]
13. Weinstein LS, Chen M, Xie T, et al. Genetic diseases associated with heterotrimeric G proteins. *Trends Pharmacol Sci.* 2006; 27:260–266. [PubMed: 16600389]
14. Weinstein LS, Xie T, Zhang Q-H, et al. Studies of the regulation and function of the Gs alpha gene Gnas using gene targeting technology. *Pharmacol Ther.* 2007; 115:271–291. [PubMed: 17588669]
15. Weinstein LS, Xie T, Qasem A, et al. The role of GNAS and other imprinted genes in the development of obesity. *Int J Obesity.* 2010; 34:6–17.
16. Bastepe M, Gunes Y, Perez-Villamil B, et al. Receptor-mediated adenylyl cyclase activation through XLalpha(s), the extra-large variant of the stimulatory G protein alpha-subunit. *Mol Endocrinol.* 2002; 16:1912–1919. [PubMed: 12145344]
17. Ischia R, Lovisetti-Scamihorn P, Hogue-Angeletti R, et al. Molecular cloning and characterization of NESP55, a novel chromogranin-like precursor of a peptide with 5-HT1B receptor antagonist activity. *J Biol Chem.* 1997; 272:11657–11662. [PubMed: 9111083]
18. Adegbite NS, Xu M, Kaplan FS, et al. Diagnostic and mutational spectrum of progressive osseous heteroplasia (POH) and other forms of GNAS-based heterotopic ossification. *Am J Med Genet A.* 2008; 146:1788–1796. [PubMed: 18553568]
19. Weinstein LS, Yu S, Warner DR, et al. Endocrine manifestations of stimulatory G protein alpha-subunit mutations and the role of genomic imprinting. *Endocr Rev.* 2001; 22:675–705. [PubMed: 11588148]
20. Bastepe M, Juppner H. GNAS locus and pseudohypoparathyroidism. *Horm Res.* 2005; 63:65–74. [PubMed: 15711092]
21. Pignolo RJ, Kassem M. Circulating osteogenic cells: Implications for injury, repair, and regeneration. *J Bone Miner Res.* 2011; 26:1685–1693. [PubMed: 21538513]
22. Zuk PA, Zhu M, Ashjian P, et al. Human adipose tissue is a source of multipotent stem cells. *Mol Biol Cell.* 2002; 13:4279–4295. [PubMed: 12475952]

23. Pignolo RJ, Xu MQ, Russell E, et al. Heterozygous inactivation of *Gnas* in adipose-derived mesenchymal progenitor cells enhances osteoblast differentiation and promotes heterotopic ossification. *J Bone Miner Res.* 2011; 26:2647–2655. [PubMed: 21812029]
24. Germain-Lee EL, Schwindinger W, Crane JL, et al. A mouse model of albright hereditary osteodystrophy generated by targeted disruption of exon 1 of the *Gnas* gene. *Endocrinology.* 2005; 146:4697–4709. [PubMed: 16099856]
25. Schwindinger WF, Reese KJ, Lawler AM, et al. Targeted disruption of *Gnas* in embryonic stem cells. *Endocrinology.* 1997; 138:4058–4063. [PubMed: 9322912]
26. Ishikawa A, Tanahashi T, Kodama H. A proximal genomic region of mouse chromosome 10 contains quantitative trait loci affecting fatness. *Anim Sci J.* 2011; 82:209–214. [PubMed: 21729197]
27. Lebrun M, Richard N, Abeguile G, et al. Progressive osseous heteroplasia: A model for the imprinting effects of *GNAS* inactivating mutations in humans. *J Clin Endocrinol Metab.* 2010; 95:3028–3038. [PubMed: 20427508]
28. Yu ZK, Wright JT, Hausman GJ. Preadipocyte recruitment in stromal vascular cultures after depletion of committed preadipocytes by immunocytotoxicity. *Obes Res.* 1997; 5:9–15. [PubMed: 9061710]
29. Huso DL, Edie S, Levine MA, et al. Heterotopic ossifications in a mouse model of albright hereditary osteodystrophy. *PLoS One.* 2011; 6:e21755. [PubMed: 21747923]
30. Farmer SR. Transcriptional control of adipocyte formation. *Cell Metab.* 2006; 4:263–273. [PubMed: 17011499]
31. Kim HB, Kim WH, Han KL, et al. cAMP-response element binding protein (CREB) positively regulates mouse adiponectin gene expression in 3T3-L1 adipocytes. *Biochem Biophys Res Commun.* 2010; 391:634–639. [PubMed: 19932681]
32. Tang QQ, Jiang MS, Lane MD. Repressive effect of Sp1 on the C/EBP alpha gene promoter: Role in adipocyte differentiation. *Mol Cell Biol.* 1999; 19:4855–4865. [PubMed: 10373535]
33. Wang HY, Watkins DC, Malbon CC. Antisense oligonucleotides to G (s) protein alpha-subunit sequence accelerate differentiation of fibroblasts to adipocytes. *Nature.* 1992; 358:334–337. [PubMed: 1379345]
34. Zhang L, Paddon C, Lewis MD, et al. Gs alpha signalling suppresses PPAR gamma 2 generation and inhibits 3T3L1 adipogenesis. *J Endocrinol.* 2009; 202:207–215. [PubMed: 19460852]
35. Chen M, Gavrilova O, Liu J, et al. Alternative *Gnas* gene products have opposite effects on glucose and lipid metabolism. *Proc Natl Acad Sci USA.* 2005; 102:7386–7391. [PubMed: 15883378]
36. Yu S, Castle A, Chen M, et al. Increased insulin sensitivity in Gsalpha knockout mice. *J Biol Chem.* 2001; 276:19994–19998. [PubMed: 11274197]
37. Yu S, Gavrilova O, Chen H, et al. Paternal versus maternal transmission of a stimulatory G-protein alpha subunit knockout produces opposite effects on energy metabolism. *J Clin Invest.* 2000; 105:615–623. [PubMed: 10712433]
38. Plagge A, Gordon E, Dean W, et al. The imprinted signaling protein XL alpha s is required for postnatal adaptation to feeding. *Nat Genet.* 2004; 36:818–826. [PubMed: 15273686]
39. Xie T, Plagge A, Gavrilova O, et al. The alternative stimulatory G protein alpha-subunit XLalphas is a critical regulator of energy and glucose metabolism and sympathetic nerve activity in adult mice. *J Biol Chem.* 2006; 281:18989–18999. [PubMed: 16672216]
40. Clark CA, Li TF, Kim KO, et al. Prostaglandin E2 inhibits BMP signaling and delays chondrocyte maturation. *J Orthop Res.* 2009; 27:785–792. [PubMed: 19023895]
41. Nakao Y, Koike T, Ohta Y, et al. Parathyroid hormone enhances bone morphogenetic protein activity by increasing intracellular 3', 5'-cyclic adenosine monophosphate accumulation in osteoblastic MC3T3-E1 cells. *Bone.* 2009; 44:872–877. [PubMed: 19442611]
42. Ohta Y, Nakagawa K, Imai Y, et al. Cyclic AMP enhances smad-mediated BMP signaling through PKA-CREB pathway. *J Bone Min Metab.* 2008; 26:478–484.
43. Siddappa R, Martens A, Doorn J, et al. cAMP/PKA pathway activation in human mesenchymal stem cells in vitro results in robust bone formation in vivo. *Proc Natl Acad Sci USA.* 2008; 105:7281–7286. [PubMed: 18490653]

44. Teplyuk NM, Galindo M, Teplyuk VI, et al. Runx2 regulates G protein-coupled signaling pathways to control growth of osteoblast progenitors. *J Biol Chem.* 2008; 283:27585–27597. [PubMed: 18625716]
45. Tsutsumimoto T, Wakabayashi S, Kinoshita T, et al. A phosphodiesterase inhibitor, pentoxifylline, enhances the bone morphogenetic protein-4 (BMP-4)-dependent differentiation of osteoprogenitor cells. *Bone.* 2002; 31:396–401. [PubMed: 12231412]
46. Zhao L, Yang S, Zhou GQ, et al. Downregulation of cAMP-dependent protein kinase inhibitor gamma is required for BMP-2-induced osteoblastic differentiation. *Int J Biochem Cell Biol.* 2006; 38:2064–2073. [PubMed: 16870489]
47. Hong SHH, Lu XH, Nanes MS, et al. Regulation of osterix (Osx, Sp7) and the Osx promoter by parathyroid hormone in osteoblasts. *J Mol Endocrinol.* 2009; 43:197–207. [PubMed: 19505977]
48. Yang D-C, Tsay H-J, Lin S-Y, et al. cAMP/PKA regulates osteogenesis, adipogenesis and ratio of RANKL/OPG mRNA expression in mesenchymal stem cells by suppressing leptin. *PLoS One.* 2008; 3:e1540. [PubMed: 18253488]
49. Zhang S, Xu M, Kaplan FS, et al. G protein-cAMP pathway regulates early stage embryonic stem cell-derived osteoblast differentiation. *J Bone Miner Res.* 2009; 24:S115.
50. Zhao Y, Ding S. A high-throughput siRNA library screen identifies osteogenic suppressors in human mesenchymal stem cells. *Proc Natl Acad Sci USA.* 2007; 104:9673–9678. [PubMed: 17535907]

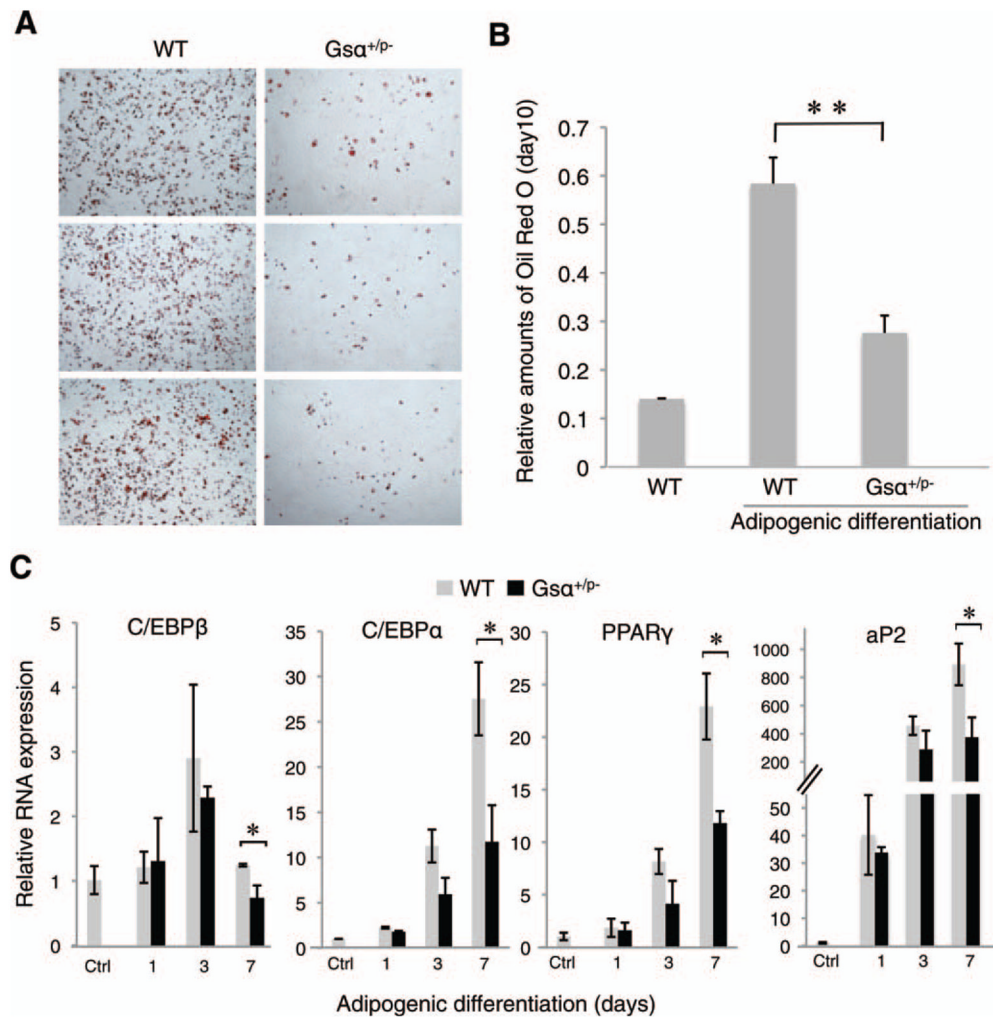


**Figure 1.** Paternally inherited *Gsa* mutation impairs adipogenesis in vitro. **(A, B):** Adipose stromal cells (ASCs) from subcutaneous fat pads from *Gsa*<sup>+/*p*-</sup> or WT mice were cultured under adipogenic conditions for 7 days then stained with oil red O and quantified at OD<sub>500</sub>. \*\*,  $p < .01$ . **(C):** Quantitative reverse-transcriptase polymerase chain reaction analysis of adipogenic markers in ASCs from fat pads on days 1, 3, and 7 after adipogenic induction. \*,  $p < .05$ . Four independent experiments used cells from three WT and three mutant mice (analyzed individually, in triplicate) for each experiment. Abbreviations: aP2, adipocyte protein 2; C/EBP, CCAAT-enhancer-binding protein; PPAR, peroxisome proliferator-activated receptor; WT, wild type.



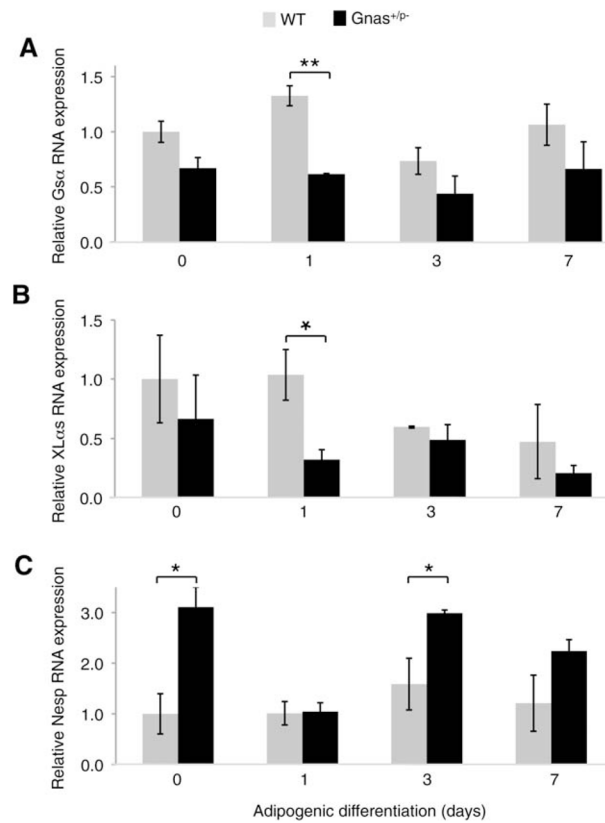


**Figure 2.**

Expression of *Gnas* transcripts during adipocyte differentiation. Quantitative reverse-transcriptase polymerase chain reaction analysis of *Gnas* transcripts *Gsa* (A), *XLas* (B), and *Nesp* (C) in fat pad-derived adipose stromal cells from *Gsa*<sup>+/-</sup> and WT mice on days 1, 3, and 7 after induction of adipogenesis. \*\*,  $p < .01$  and \*,  $p < .05$ . Three independent experiments used cells from three WT and three mutant mice (analyzed individually, in triplicate) for each experiment. Abbreviations: *Gsa*, guanine nucleotide-binding protein G(s) subunit alpha; *Nesp*, neuroendocrine secretory protein of mol. wt. 55,000; WT, wild-type; *XLas*, guanine nucleotide-binding protein G(s) subunit alpha extralarge isoform.



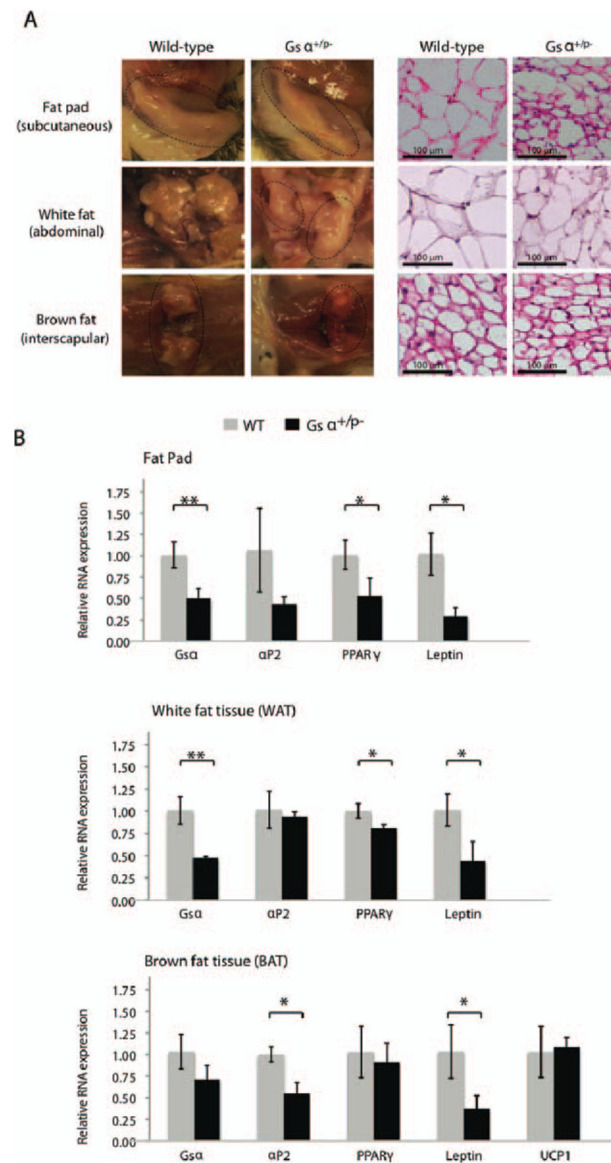


**Figure 4.** Inactivating *Gsα* mutation reduces adipogenic tissues in vivo. **(A):** Adipose tissues from subcutaneous fat pads, abdominal white fat, and interscapular brown fat from *Gsα*<sup>+/-</sup> ( $n = 3$ ) and WT ( $n = 3$ ) mice (left panels) were examined histologically with hematoxylin and eosin staining (right panels). (Supporting Information Fig. 2). **(B):** Expression of adipose markers was quantified using reverse-transcriptase polymerase chain reaction. \*,  $p < .05$ ; \*\*,  $p < .01$ . Three independent experiments used cells from three WT and three mutant mice (analyzed individually in triplicate) for each experiment. Abbreviations:  $\alpha$ P2, adipocyte protein 2; PPAR, peroxisome proliferator-activated receptor; UCP1, uncoupling protein 1; WT, wild type.

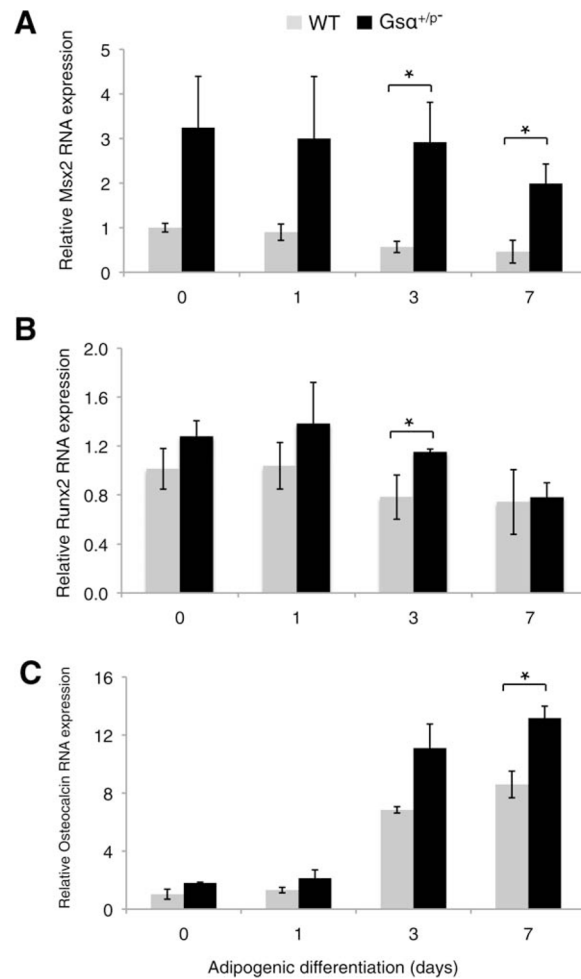


**Figure 5.** Paternally inherited *Gsa* mutation potentiates osteogenesis during adipogenic induction. Expression of the osteogenic markers, Msx2 (**A**), Runx2 (**B**), and Osteocalcin (**C**) were detected by quantitative reverse-transcriptase polymerase chain reaction (qRT-PCR) in adipose stromal cells from fat pads of *Gsa*<sup>+/p-</sup> and WT mice grown under adipogenic differentiation conditions. Samples were analyzed by qRT-PCR on days 0, 1, 3, and 7. \*,  $p < .05$ . Three independent experiments used cells from three WT and three mutant mice (analyzed individually in triplicate) for each experiment. Abbreviations: Msx2, msh homeobox 2; Runx2, runt-related transcription factor 2; WT, wild type.

Table 1

Anthromorphometric and gross adipose tissue measurements

Genotype	Total mouse weight (g)	Length (cm)	BMI (g/cm <sup>2</sup> )	Fat pads (g)	WAT (g)	BAT (g)
WT (n = 27)	36.91 ± 1.98	9.55 ± 0.24	0.41 ± 0.02	0.88 ± 0.24	0.87 ± 0.22	0.20 ± 0.03
KO (n = 16)	29.66 ± 1.25 <sup>***</sup>	8.94 ± 0.24 <sup>***</sup>	0.37 ± 0.03 (N.S.)	0.44 ± 0.08 <sup>***</sup>	0.35 ± 0.08 <sup>***</sup>	0.11 ± 0.03 <sup>***</sup>

All values are average ± SD.

<sup>\*\*\*</sup>  $p < .001$ , two-sided  $t$  test  $Gs\alpha^{+}/p^{-}$  (KO) versus WT mice.

Abbreviations: BAT, brown adipose tissue; BMI, body mass index; KO, knockout; N.S., not significant; WAT, white adipose tissue; WT, wild type.



**Table 2**

Histomorphometric analysis of adipose tissues

	<i>N</i> (no. cells counted)	Mean cell size ( $\mu\text{m}^2$ )	% stroma	Adipocyte number per 10,000 $\mu\text{m}^2$
FP				
WT	254	1704 $\pm$ 425	28 $\pm$ 3.8	4 $\pm$ 1.1
KO	544	642 $\pm$ 87.9 <sup>***</sup>	36 $\pm$ 3.3 <sup>**</sup>	10 $\pm$ 1.8 <sup>***</sup>
WAT				
WT	212	2853 $\pm$ 512	31 $\pm$ 3.6	2.4 $\pm$ 0.53
KO	635	1883 $\pm$ 332 <sup>***</sup>	31 $\pm$ 5.8	3.7 $\pm$ 0.78 <sup>***</sup>
BAT				
WT	784	319 $\pm$ 53	44 $\pm$ 7.2	17 $\pm$ 2.8
KO	435	259 $\pm$ 25.8 <sup>*</sup>	45 $\pm$ 5.4	21 $\pm$ 3.3 <sup>*</sup>

All values are average  $\pm$  SD.

\*  $p < .05$ ;

\*\*  $p < .01$ ;

\*\*\*  $p < .001$ ; two-sided *t* test  $G\alpha^{+/P-}$  (KO) versus WT mice.

Abbreviations: BAT, brown adipose tissue; FP, fat pads; KO, knockout; WAT, white adipose tissue; WT, wild type.